

Ferromagnetic order in a cuprate superconductor

Tarapada Sarkar, P. R. Mandal, Nicholas R. Poniatowski and Richard L. Greene

Center for Nanophysics & Advanced Materials and Department of Physics, University of Maryland, College Park, Maryland 20742, USA.

Abstract

The unexplained normal state and superconducting (SC) properties of the cuprates are believed to arise from doping an antiferromagnetic (AFM) Mott insulator. The competition between the AFM and SC can explain the increase in the SC transition temperature (T_c) with doping. However, the decrease in T_c beyond optimal doping remains an outstanding enigma. Here, we use resistivity, magnetothermopower and magnetization experiments to show the emergence of a ferromagnetic (FM) phase beyond the superconducting dome in the electron-doped cuprate $\text{La}_{2-x}\text{Ce}_x\text{CuO}_4$ (LCCO). This unexpected discovery suggests that a quantum phase transition occurs at the end of the SC dome and that a competition between superconductivity and FM can explain the decrease in T_c in the over doped cuprates. Our findings show that the overdoped cuprates are not as simple as previously thought and they pose a challenge to most models proposed for the cuprates.

The physics of the copper oxide (cuprate) superconductors has been intensely debated since their discovery in 1986. Although the physics of a doped Mott insulator can explain many properties of the underdoped and optimal doped cuprates, it is not clear how this approach can work at higher dopings. In fact, it is usually assumed that over-doped cuprates are very conventional and that they emerge from a Fermi liquid (FL) normal state. But, recent work has found a non-Fermi liquid (strange metal) normal state, with a linear-in-T resistivity down to 30 mK, in overdoped LCCO (1). Another result finds an unconventional (non-FL) linear-in-H magnetoresistance in LCCO (2), correlated with the linear-in-T resistivity and the disappearance of SC for doping above the Fermi surface reconstruction at $x=0.14$ (3). Moreover, an unconventional thermoelectric power is observed in the same region of the LCCO phase diagram (4). All these experiments indicate that the nature of the normal state at low temperatures in the overdoped region is a non-Fermi liquid with a possible extended doping range of quantum criticality. Similar observations of non-FL transport have also been reported for the overdoped p-

type cuprate $\text{La}_{2-x}\text{Sr}_x\text{CuO}_4$ (LSCO), down to 4K (5). Moreover, an anomalous loss of superfluid density has been observed in overdoped LSCO (6)

In 2007, Kopp et al. (7) hypothesized that the temperature dependence of the magnetic susceptibility (χ) in overdoped $(\text{Bi, Pb})_2\text{Sr}_2\text{CuO}_{6+\delta}$ is caused by the fluctuations of a FM phase that exists beyond the end of the superconducting dome and which competes with the d-wave superconductivity. Competition with ferromagnetic order is a potential explanation for the vanishing superconductivity in the overdoped side of the phase diagram of the cuprates and the loss of superfluid density. The proposal for ferromagnetic order at high charge doping is supported by electronic band calculations for super cells of $\text{La}_{2-x}\text{Ba}_x\text{CuO}_4$ (8), which predict weak ferromagnetism around concentrated regions of the Ba-dopant atom at very low temperatures. In 2010, Sonier et al. (9) reported development of ferromagnetic fluctuations below 0.9 K in non-superconducting and heavily overdoped LSCO. Recently, K. Kurashima et al. (10) have found some evidence for ferromagnetic fluctuations in overdoped $(\text{Bi, Pb})_2\text{Sr}_2\text{CuO}_{6+\delta}$. However, to date, there is no direct experimental evidence of static ferromagnetic order in any cuprate.

Most prior studies of cuprates have been focused on doping within the superconducting dome and little attention has been paid to the region beyond the SC dome due to difficulties in preparing heavily overdoped samples. To investigate the magnetic properties of highly overdoped cuprate superconductors, we have measured electron-doped LCCO films, which can be doped beyond the superconducting dome. Here we focus on non-SC overdoped LCCO ($x=0.18$ and 0.19), where a FL quadratic temperature dependent resistivity is found at low temperatures (1). The surprising new result is the observation of static ferromagnetic order at temperatures below 4 K. No ferromagnetic order is found for doping inside the superconducting dome ($x<0.175$). Our work strongly suggests the existence of a ferromagnetic quantum critical point at the end of the dome at $x=0.175$. This can explain the previously reported (11) field-induced quantum critical behavior at the end of the superconducting dome and possibly the decrease of the superconductivity as doping is increased beyond the optimal doping.

The evidence for FM order below 4K in overdoped (non-SC) LCCO is based on transport and magnetization measurements that are unequivocal indicators of FM in known FM metals.

These are negative transverse magnetoresistance (MR), magnetic field hysteresis in magnetization, MR, and magnetothermopower and anisotropic MR. In Fig. 1 we show the transverse magnetoresistance at a few low temperatures for a SC film ($x=0.17$) and a non-SC film ($x=0.18$). The MR for $x=0.17$ is positive and has a crossover from linear to quadratic in field with increasing temperature. In contrast, the transverse MR for $x=0.18$ is negative with a strong low field hysteric dependence below ~ 4 K. The negative MR and low field hysteresis below 4 K is very strong evidence for static ferromagnetism (12). Similar FM-like MR is shown in Fig. 2a (and b) for $x=0.19$, again below ~ 4 K. In addition, as shown in Fig. 2d, we observed hysteresis in the magnetothermoelectricpower (MTEP) (13,14), which rules out any current heating effect as the cause of the MR hysteresis. In Fig. 2c we show a SQUID magnetization (M) study of the $x=0.19$ film that gives a M vs H hysteresis below 4 K, with a coercive field comparable to the MR shown in Fig. 2(a,b). The hysteresis vanishes at 4K as shown in Fig. S3. The magnetization exhibits an in-plane, out of -plane anisotropy, as shown in Fig. 2c. The magnitude of the magnetization at 2 K is approximately $\sim 0.06-0.08 \mu_B/fu$. This is consistent with weak metallic ferromagnetism from the copper spins. We can rule out an extrinsic origin for the ferromagnetism, as discussed in detail in the SI.

The negative transverse MR, along with hysteretic MR, MTEP and magnetization are unambiguous indicators of static FM below 4K in overdoped LCCO. In further support of this, we find an anisotropic magnetoresistance (AMR), which is a well-known effect in metallic ferromagnets and is a consequence of spin orbit coupling [12,15-18]. The data is shown in Fig. 1(b,c) and Fig. 3, where the MR depends on the relative orientation of the current and the magnetization.

We find that the transverse MR remains negative up to ~ 70 K (Fig. S2). Based on prior experiments on low carrier density ferromagnetic transition metals (19), and theory (20), we would guess that ferromagnetic fluctuations are present. However, we did not observe evidence of FM spin fluctuations in the temperature dependence of the resistivity, which follows T^2 behavior up to ~ 100 K, rather than a $T^{4/3}$ (2D) or $T^{5/3}$ (3D) behavior predicted for FM fluctuations (21). Future experiments such as uSR (9,10) will be needed to probe the range and impact of the FM fluctuations. The FM in overdoped, non-SC, LCCO resembles that found in

weak itinerant ferromagnets such as UGe_2 (22) and Y_4Co_3 (23), which also exhibit T^2 resistivity. The FM order may exist above the doping $x=0.19$, but we were unable to prepare homogeneous films. The onset of SC at 5 K for $x=0.17$ rules out a low temperature MR study for this doping. Based on the positive normal state MR in $x=0.17$ (shown in Fig.1) and the uSR study of LCCO (24), it is reasonable to predict the absence of any FM order below $x=0.175$. We attribute the observed ferromagnetism to the hypothesized low temperature ferromagnetic order in the copper oxide planes of overdoped cuprates (7).

Finally, our discovery of low temperature static FM order explains the cause of the unknown quantum critical behavior previously found at the end of the SC in LCCO (11) based upon magnetic field and temperature scaling of the resistivity. These authors also reported a resistivity proportional to $T^{1.6}$ at the end of the SC dome. This power law of resistivity is close to that expected from three-dimensional FM fluctuations (21). Thus, the $T^{1.6}$ resistivity and our present result of FM order above the SC dome strongly suggests a SC to FM quantum critical point at the end of the superconducting dome in LCCO (and probably for all cuprates).

In conclusion, our present study establishes that static ferromagnetic order exists in the overdoped, non-SC, cuprate LCCO at temperatures below 4 K. This strongly suggests that there is a ferromagnetic quantum critical point at the end of the superconducting dome. Our findings support the theoretical picture of a competition between d-wave superconductivity and ferromagnetism (7), which can explain the decrease in superconductivity above optimal doping. The competition between FM and SC might also explain the loss of superfluid density recently found in hole-doped cuprates (6). Our surprising results provide an important new clue to solve the mystery of the cuprate superconductors.

Methods:

High quality $\text{La}_{2-x}\text{Ce}_x\text{CuO}_4$ (LCCO) thin films of thickness about 150 - 200 nm were grown using the pulsed laser deposition (PLD) technique on SrTiO_3 [100] substrates as in our previous work (2) The LCCO targets were prepared by the solid-state reaction method using 99.999% pure La_2O_5 , CeO_5 , and CuO powders. The magnetotransport measurements have been

carried out in a Quantum Design Physical Property Measurement System. The magnetization measurement was done in a superconducting quantum interference device (SQUID) equipped with a 7 T magnet. The thermopower measurement is done with single heater technique (ref 4, main text).

Acknowledgements: This work is supported by the NSF under Grant No.DMR-1708334 and the Maryland Center for Nanophysics and Advanced Materials (CNAM). We thank Johnpierre Paglione, Nick Butch, Wesley Fuhrman, and Joshua Higgins for very helpful discussions and comments on the manuscript.

Author contributions:

R.L.G directed the project. T.S performed the analysis and the MR and magnetization measurements. P.R.M performed the thermoelectric measurement. T.S and N. R. P prepared the samples. R.L.G and T.S wrote the manuscript and discussed with all other authors.

Additional information:

Supplementary information is available in the online version of the paper. Reprints and Permission information is available online at

Correspondence and requests for materials should be addressed to R. L. G.

Competing financial interests:

The authors declare no competing financial interests.

References:

1. K. Jin, et al., Link between spin fluctuations and electron pairing in copper oxide superconductors. *Nature*, **476**, 73 (2011).
2. T. Sarkar, P. R. Mandal, N. R. Poniatowski, MK Chan, R. L. Greene, Correlation between scale-invariant normal state resistivity and superconductivity in an electron-doped cuprate, arXiv:**1810.03499** (2018).
3. T. Sarkar, et al., Fermi surface reconstruction and anomalous low-temperature resistivity in electron-doped $\text{La}_{2-x}\text{Ce}_x\text{CuO}_4$. *Phys. Rev. B* **96**, 155449 (2017).
4. P. R. Mandal, T. Sarkar, R. L. Greene, Anomalous quantum criticality in the electron-doped cuprates. arXiv:**1810.06511** (2018).
5. R. A. Cooper, et al. Anomalous Criticality in the Electrical Resistivity of $\text{La}_{2-x}\text{Sr}_x\text{CuO}_4$. *Science* **323**, 603 (2009).
6. I. Božović, X. He, J. Wu and A. T. Bollinger, Dependence of the critical temperature in overdoped copper oxides on superfluid density. *Nature* **536**, 309–311 (2016).
7. A. Kopp, A. Ghosal, S. Chakravarty, Competing ferromagnetism in high-temperature copper oxide superconductors. *Proc Natl Acad Sci*, **104**, 6123–6127, (2007)
8. B. Barbiellini, T. Jarlborg, Importance of local band effects for ferromagnetism in hole-doped La_2CuO_4 cuprate superconductors. *Phys. Rev. Lett.* **101**, 157002 (2008).

9. J. E. Sonier, C. V. Kaiser, V. Pacradouni, S. A. Sabok-Sayr, C. Cochrane, D. E. MacLaughlin, S. Komiya, and N. E. Hussey, *Proc. Natl. Acad. Sci.* **107**, 17131 (2010).
10. Koshi Kurashima et al. Development of Ferromagnetic Fluctuations in Heavily Overdoped $(\text{Bi,Pb})_2\text{Sr}_2\text{CuO}_{6+\delta}$ Copper Oxide, *Phys. Rev. Lett.* **121**, 057002 (2018).
11. N. Butch and K. Jin et al., Quantum critical scaling at the edge of Fermi liquid stability in a cuprate superconductor, *PNAS*, **109**, 8440-8444 (2012).
12. M. Viret et al. Spin scattering in ferromagnetic thin films, *Phys. Rev. B.* **53**, 13 (1995).
13. Y. Pu et al., Anisotropic Thermopower and Planar Nernst Effect in $\text{Ga}_{1-x}\text{Mn}_x\text{As}$ Ferromagnetic Semiconductors, *PRL* **97**, 036601 (2006).
14. A. D. Avery, M. R. Pufall and B. L. Zink, Determining the planar Nernst effect from magnetic-field-dependent thermopower and resistance in nickel and permalloy thin films. *Phys. Rev. B* **86**, 184408 (2012).
15. T. R. McGuire and R. I. Potter, *IEEE Trans. Magn. Mater.* **11**, 1018 (1975).
16. Th. G. S. M. Rijks et al., In-plane and out-of-plane anisotropic magnetoresistance in $\text{Ni}_{80}\text{Fe}_{20}$ thin films, *Phys. Rev. B* **56**, 362 (1997).
17. J. F. Gregg et. al., Giant Magnetoresistive Effects in a Single Element Magnetic Thin Film, *Phys Rev Lett.* **77**, 1580 (1996).
18. L. Berger, Low-field magnetoresistance and domain drag in ferromagnets, *J. Appl. Phys.* **49**, 2156 (1978).
19. Y. Shimakawa, Y. Kubo & T. Manako, Giant magnetoresistance in $\text{Ti}_2\text{Mn}_2\text{O}_7$ with the pyrochlore structure, *Nature*, **379**, 53–55 (1996).
20. P. Majumdar, P.B. Littlewood, Magnetoresistance in Mn Pyrochlore: Electrical Transport in a Low Carrier Density Ferromagnet, *Phys. Rev. Lett.* **81**, 1314 (1998).
21. T. Moriya and K. Ueda, Antiferromagnetic spin fluctuation and superconductivity, *Rep. Prog. Phys.* **66**, 1299 (2003).
22. S. S. Saxena et al., Superconductivity on the border of itinerant-electron ferromagnetism in UGe_2 , *Nature*, **406**, 587–592 (2000).
23. A. Kolodziejczyk and J Spalek, *Journal of Physics F: Metal Physics*, **14**, 1277 (1984).
24. H. Saadaoui, et al., The phase diagram of electron-doped $\text{La}_{2-x}\text{Ce}_x\text{CuO}_{4-\delta}$. *Nat. comm* **6**, 6041 (2015).
25. N. P. Armitage, P. Fournier, and R. L. Greene, Progress and perspectives on electron-doped cuprates, *Rev. Mod. Phys.* **82**, 2421 (2010).

Figure Caption:

Figure 1: Low temperature magnetoresistance across the end of the SC dome: (a) *ab*-plane magnetoresistivity ($H \parallel c$ axis) for $x=0.17$ ($T_c=4$ K) at 2 K, 5 K and 10 K ; (b) and (c) *ab*-plane $\Delta\rho\%$ ($= \frac{\rho(H)-\rho(0)}{\rho(0)} 100$) in low field sweep from +400 Oe to -400 Oe for $H \perp ab$ - plane and for $H \parallel ab$ - plane respectively at 2 K for $x=0.18$ ($T_c=0$ K). Arrows indicate the sweeping direction of the H field. Inset: higher field *ab*-plane magnetoresistance for $H \perp ab$ - plane at 2K

Figure 2: Magneto-transport and magnetization for $x=0.19$: (a) *ab*-plane $\Delta\rho\%$ ($= \frac{\rho(H)-\rho(0)}{\rho(0)} 100$) ($H \parallel c$ axis) at 2 K; inset: low field $\Delta\rho\%$ in expanded view. Black arrows indicate the sweeping direction of the field; (b) low field *ab*-plane $\Delta\rho\%$ ($H \parallel c$ axis) at temperatures 3 K, 3.5 K and 4 K with same sweeping direction of field as shown in the Fig. 2(a) (y axis scale is the same); (c) magnetization versus magnetic field with $H \parallel ab$ -plane, and $H \perp ab$ -plane at 2 K (see SI for higher temperatures). Inset: low field magnetization in expanded view for $H \parallel ab$ -plane. The substrate background is removed in these plots; see SI for details. (d) *ab*-plane thermoelectric power with transverse sweeping field +500 Oe to -500 Oe.

Figure-3 Anisotropic magnetoresistance of $x=0.18$: (a) *ab*-plane magnetoresistance measured with field in plane and parallel to current direction ($H \parallel I$); (b) *ab*-plane transverse magnetoresistance ($H \parallel c$) with field perpendicular to current direction. The low field data is not plotted here for clarity (see Fig.1 and Fig. S1 for the low field magnetoresistance).

Figure-4: Temperature vs doping phase diagram: Schematic phase diagram of $\text{La}_{2-x}\text{Ce}_x\text{CuO}_4$. The dotted blue line represents the region in which AF (long or short range) order is observed below doping $x=0.14$ (ref. 1 and ref. 25). The yellow region represents the superconducting phase. The red area beyond the SC dome represents the static FM phase found from this work. The black arrow indicates the possible FM QCP. The green arrows indicate the three dopings studied in this work.

Figures:

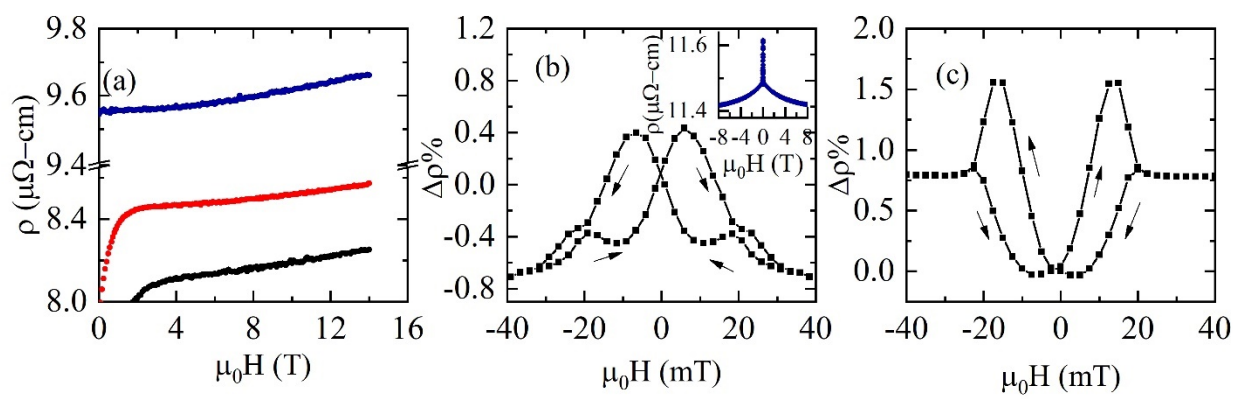


Figure-1

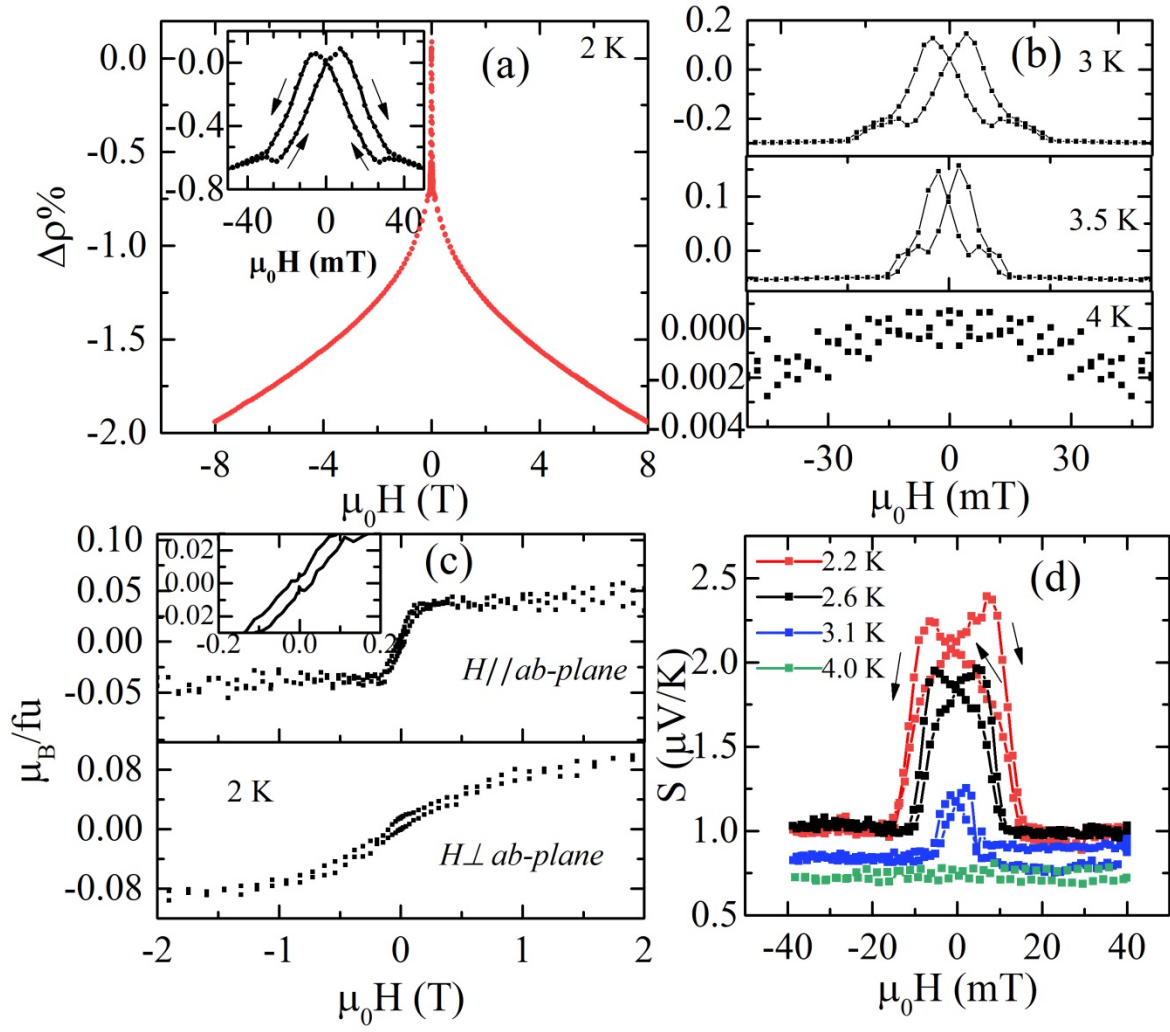


Figure-2

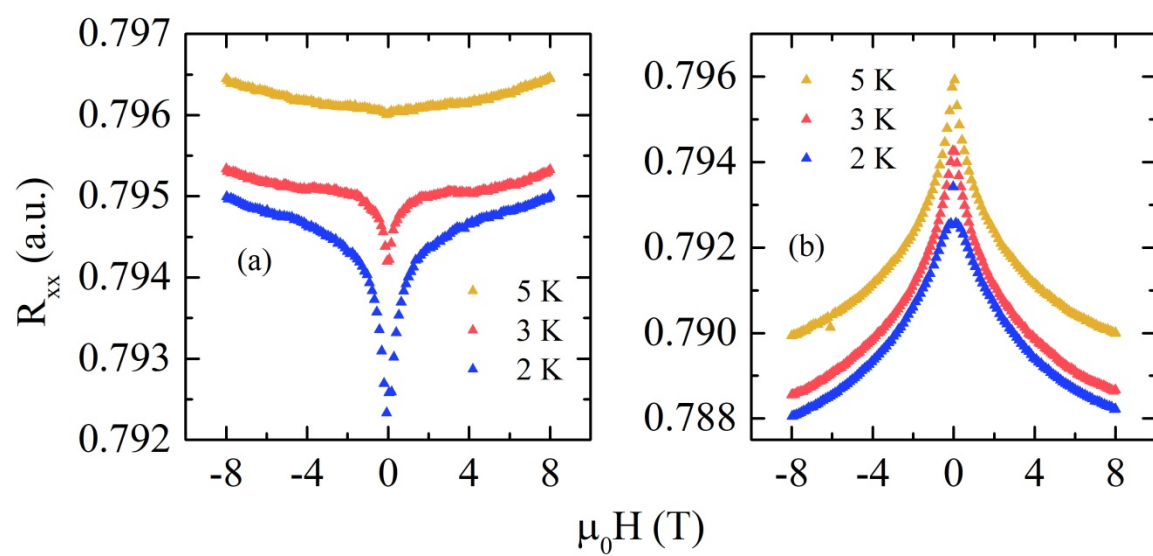


Figure-3

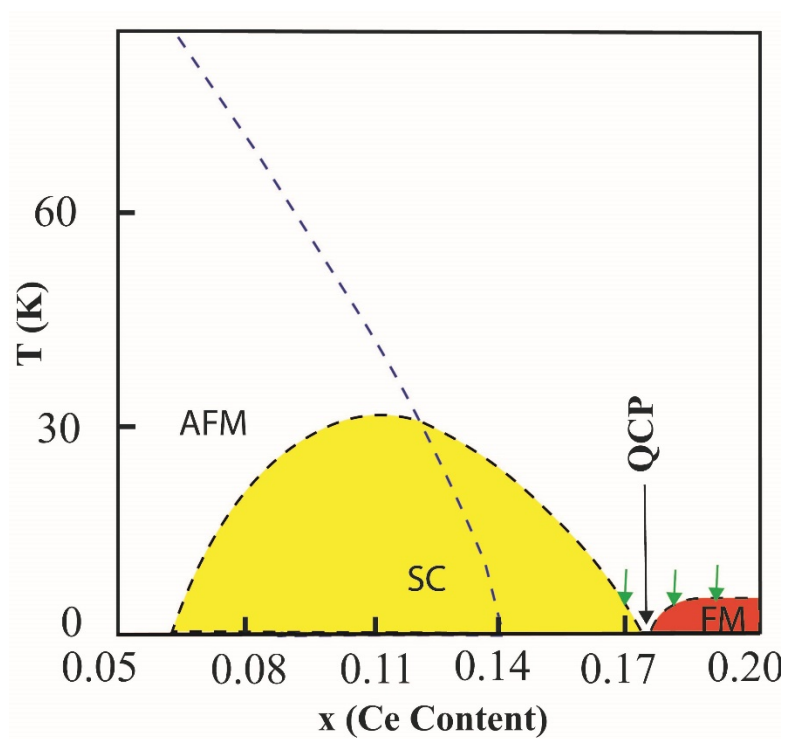


Figure-4

Supplementary Information

Low field magnetoresistance of x=0.18:

The figure S1 shows the transverse low field magnetoresistance with + 500 Oe to -500 Oe sweeping field at temperatures 2K, 3K, 3.5K and 3.7 K.

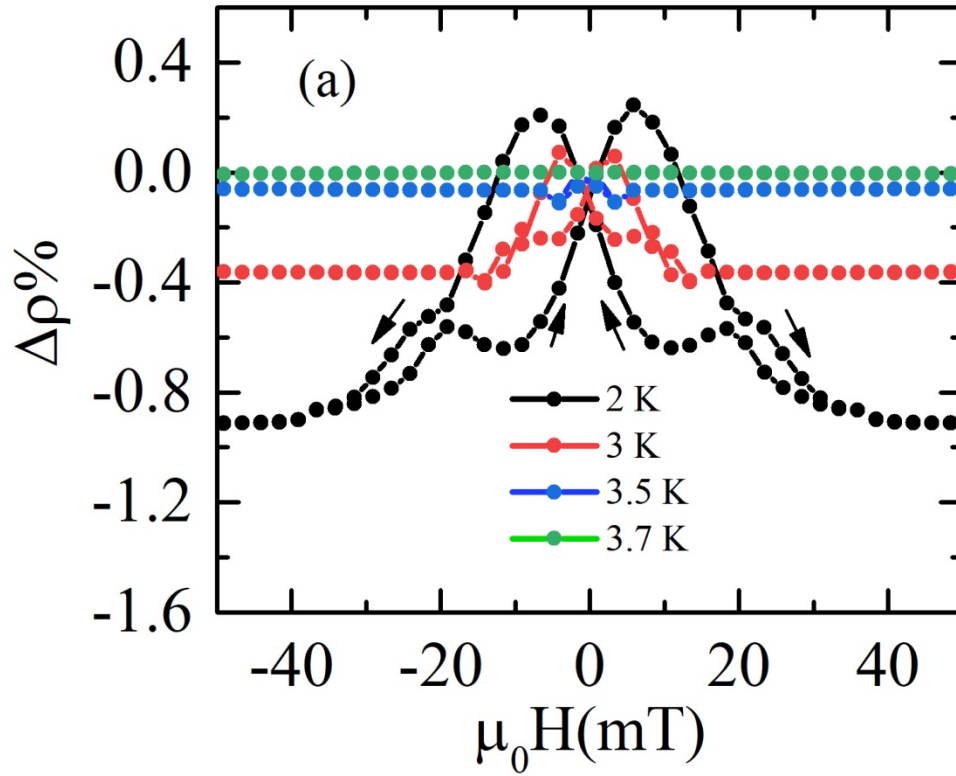


Figure S1: Low field *out-of-plane* $\Delta\rho\%$ ($= \frac{\rho(H)-\rho(0)}{\rho(0)} 100$) versus magnetic field ($H \parallel c$ axis).

High temperature magnetoresistance:

In Figure S2, we show the higher temperature out-of-plane magnetoresistance of one $x=0.18$ Ce doped LCCO sample. The MR of this sample is negative at lower temperatures below 50 K. At 50 K the low field (below 6 T) magnetoresistance is negative and at higher field it is positive. The magnetoresistance with temperatures becomes fully positive at 70 K as shown in the Fig.S2

inset. The theory for magnetoresistance in ferromagnetic metals below the Curie temperature is well understood (1). The negative magnetoresistance above the Curie temperature in a ferromagnetic metal is not common. Experimentally, negative magnetoresistance is seen in several ferromagnetic transition metals with low carrier density (main text ref-20). These observations have been explained by spin fluctuations above the Curie temperature. Cuprates are also known to be a disordered low carrier system. Based on these observations, we speculate that the negative magnetoresistance is due to ferromagnetic spin fluctuations above the ferromagnetic transition temperature (main text Fig.4).

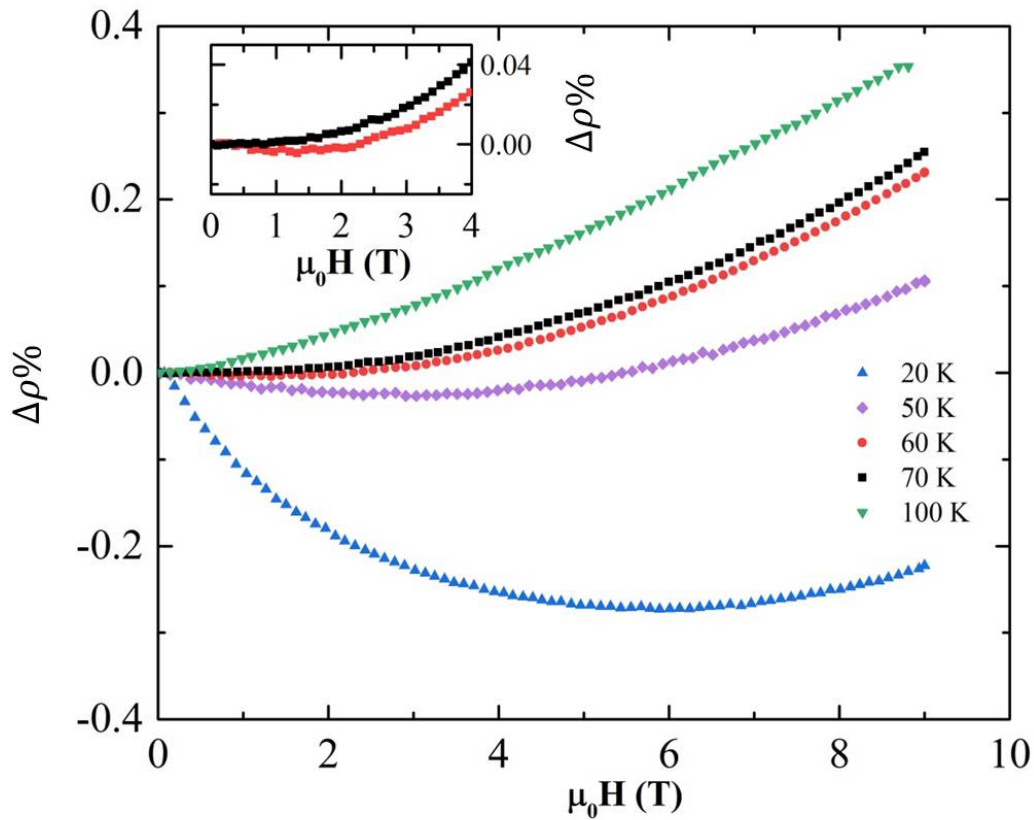
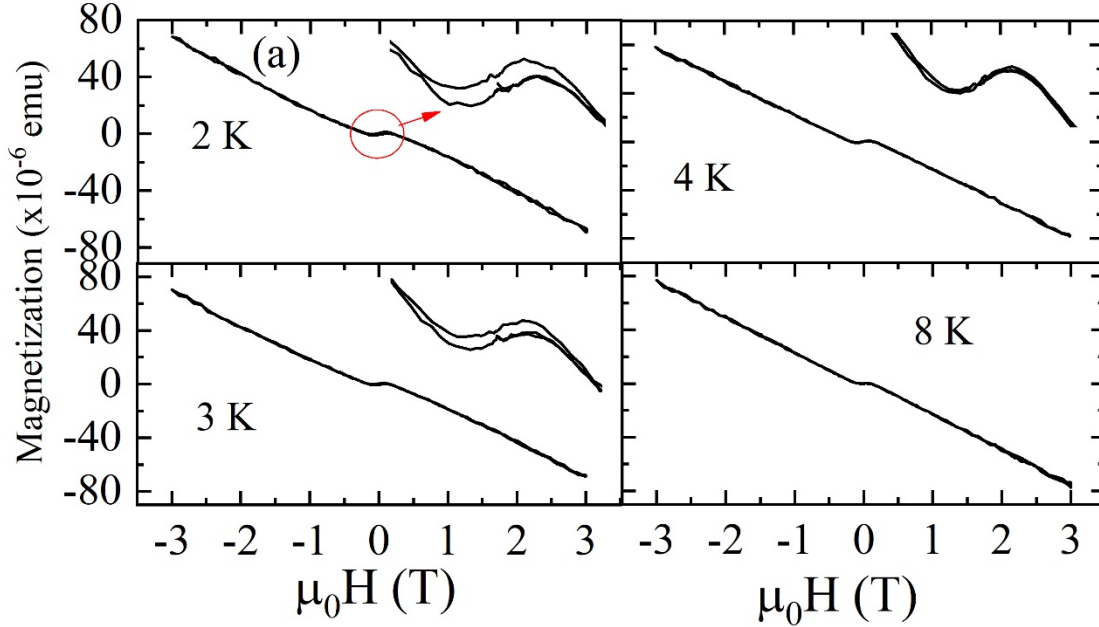


Figure-S2: Magnetoresistance: Transverse $\Delta\rho\%$ ($= \frac{\rho(H)-\rho(0)}{\rho(0)} 100$) of $x=0.18$ at various temperatures; Inset: MR at 60 K (red) and 70 K (black).

Magnetization:

Figure S3 (a) shows the magnetization (M) vs field (H) data for doping $x=0.19$ below 10 K down to 2 K for $H//ab$ -plane. The magnetization features a hysteresis loop below 4 K and no hysteresis above 4 K, which is consistent with the magnetoresistance data where the hysteresis loop is seen only below 4 K. Fig. S3(b) shows M vs H with a similar hysteresis for $H \perp ab$ -plane with slightly higher magnetic moment than that of in-plane. These data suggest there is anisotropy in the spin alignment. The Fig.S3(c) shows the M vs H in the plane of the same substrate after removing the LCCO film by chemical etching (sample was dipped inside HNO_3 for 45 seconds). The M vs H at 2 K after subtracting out the substrate background is plotted in the main text Fig. 2c. These measurements strongly support the presence of ferromagnetic order below 4 K in LCCO and eliminate any contribution from the substrate.



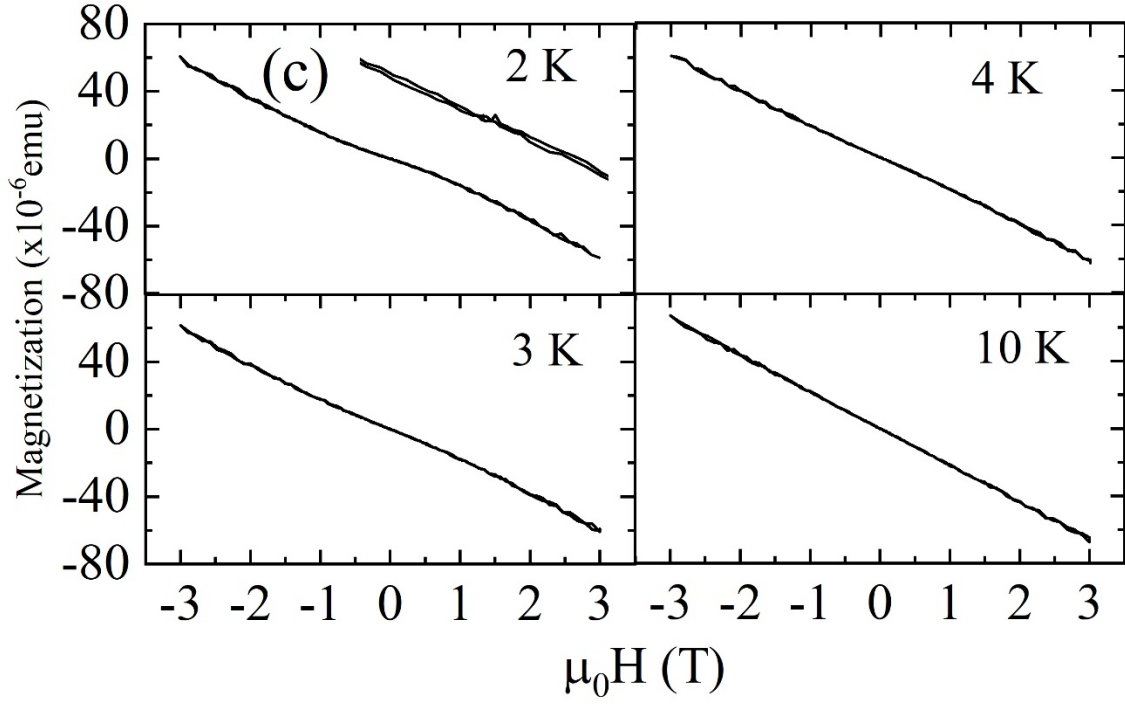
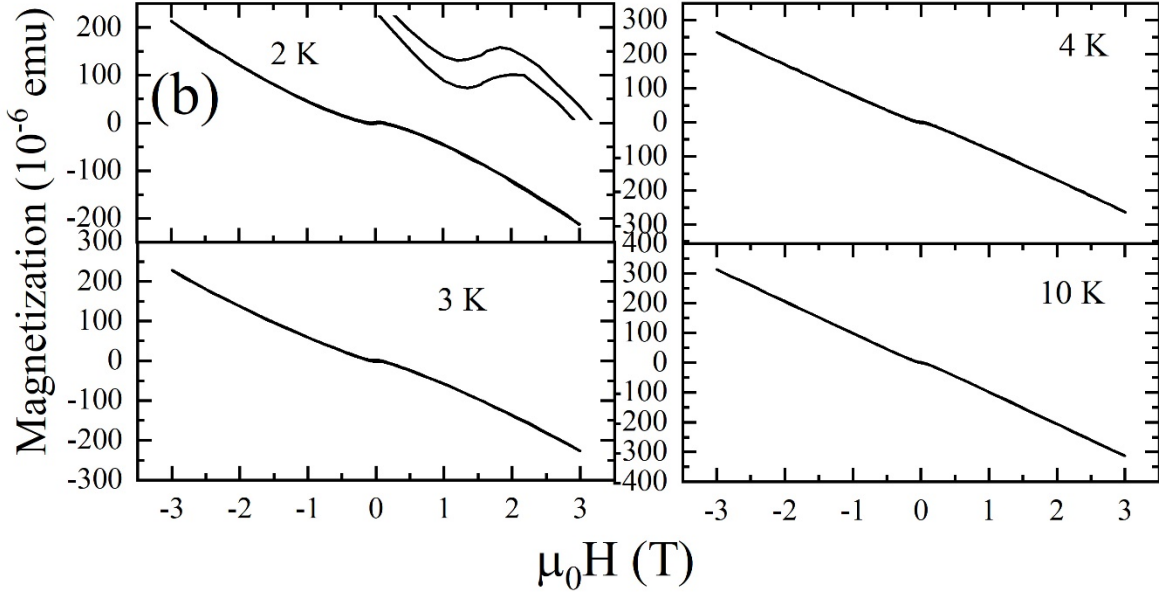


Figure S3 (a) and (b) show the M vs H of an LCCO film grown on an STO with $H//ab$ plane and $H \perp ab$ -plane respectively; (c) shows the M vs H with $H//ab$ plane after removing the film by chemical etching. Inset: low field zoom.

Magnetoresistance in other oxides:

Figure S6 shows the low field magnetoresistance of conducting Nb-SrTiO₃ and oxygen reduced SrTiO₃ metal oxides (Nb-SrTiO₃ was from CrysTec, GmbH, Germany) and oxygen reduced SrTiO₃ (2) for reduced SrTiO₃ sample preparation). The purpose of these measurements was to confirm that the low field magnetoresistance is not related to any artifact from the substrate. In the MR plotted here, we do not see any anomalous negative MR or low field hysteretic behavior. This measurement confirms that the low field magnetoresistance described in the main text is linked to the LCCO thin film rather than the substrate.

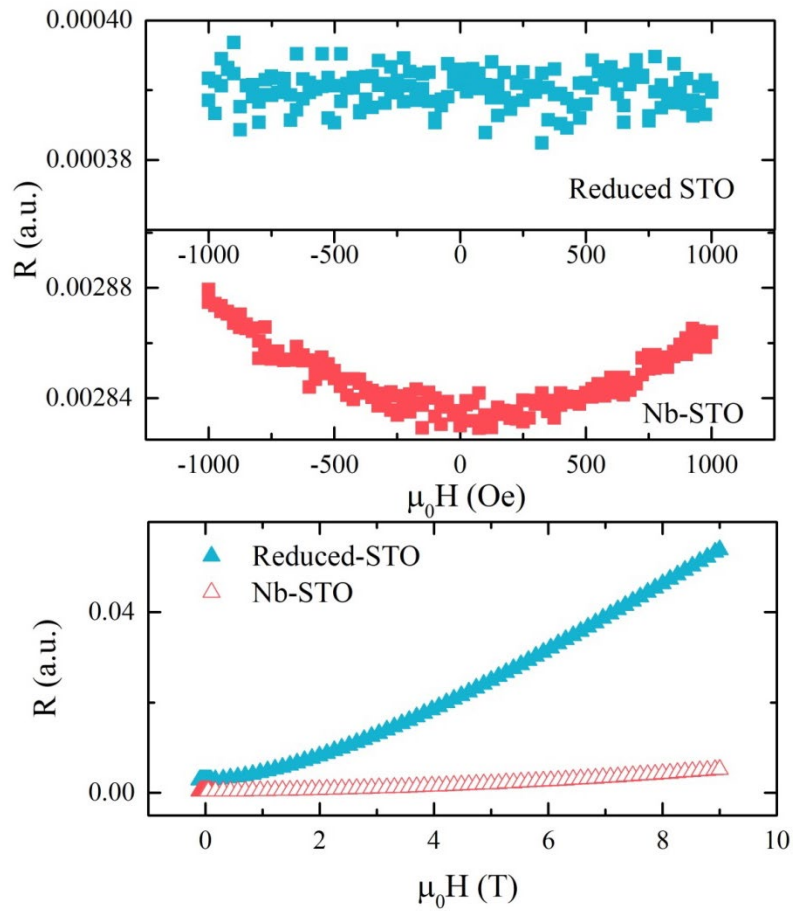


Figure-S6 Magnetoresistance of Nb-STO and reduced STO: Low field ab-plane magnetoresistance for reduced STO (top panel) and Nb-STO middle panel. Lower panel shows the measurement up to 9 T.

Intrinsic origin of the ferromagnetism:

Ferromagnetism in a thin film (below 200 nm) grown on a substrate has often been linked to a magnetic impurity origin (3). There are several possible sources of impurity ferromagnetism:

- 1) The hysteresis in a SQUID magnetometry measurement could be from contamination by sample handling with a magnetic tweezer. However, this is unlikely to show a hysteresis in magnetoresistance or magnetothermopower as we have observed.
- 2) The presence of magnetic impurities (e.g., Fe, Co, Mn) in the film or the substrate.

Our data rule this out for the following reasons:

- a) The magnitude of the magnetic moment our LCCO film is too large ($0.08 \mu_B/\text{fu}$) to be caused by magnetic impurities. A moment this large would require more than 2% of ferromagnetic impurities (like Fe, Co, Mn), which is not possible with the purity of our PLD materials.
- b) We have measured the magnetic moment in the film after subtracting out the substrate contribution (Fig-2c in the main text, Fig.S3).
- c) The slightly lower doped $x=0.17$ shows no ferromagnetic-like magnetoresistance, even though these films are prepared from same source of metal oxide.
- d) To the author's knowledge, all magnetic impurities related to weak ferromagnetism have a high Curie temperatures (above 300 K) and the saturation magnetism does not change with temperature significantly (3, 4). In contrast, the magnetism in LCCO is seen at very low temperature (below 4 K).

LCCO did not show any structural change in the X-Ray Diffraction (XRD) pattern of the higher doped sample as shown in Fig. S7. The XRD pattern looks very similar throughout the doping range studied. A recent Cu L-edge resonant inelastic X-ray scattering study (5) of LCCO shows that Cu is in the $2+$ state beyond the superconducting dome and Ce is known to be in $4+$ states (6) in electron-doped cuprates. The Ce^{4+} and La^{3+} are unlikely to be ferromagnetic (no unpaired electrons and no evidence found to date). However, we

cannot rule out a small amount (1% or less) of Ce^{3+} . But, we would not get our large measured moment from a few percent of Ce^{3+} in isolation, or combined with oxygen.

Therefore, we attribute our observed ferromagnetism to an intrinsic property of the copper spins in a metallic system, i.e., a weak metallic ferromagnet.

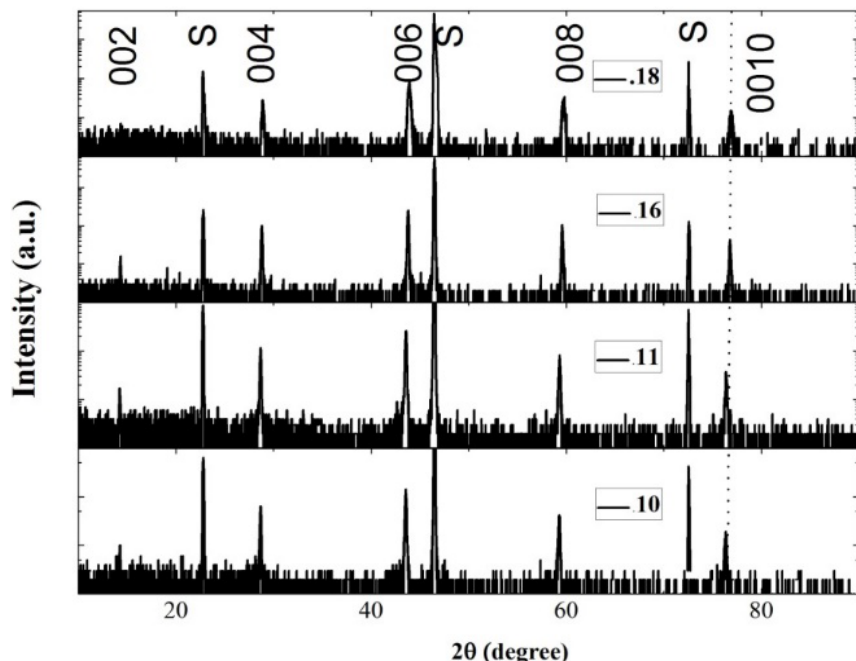


Figure S7. X-ray Diffraction pattern of $\text{La}_{2-x}\text{Ce}_x\text{CuO}_4$ grown on SrTiO_3 substrate. The S indicates substrate peak. Dopings are indicated in each panel.

References:

1. J. M. D. Coey, "Magnetotransport" in Magnetism and Magnetic Materials (Cambridge University Press, Cambridge CB2 8RU, UK (2009).
2. Z. Q. Liu et al., Magnetic-field induced resistivity minimum with in-plane linear magnetoresistance of the Fermi liquid in SrTiO_{3-x} single crystals, *Phys. Rev. B* **85**, 155114 (2012)
3. M. Khalid, A. Setzer, M. Ziese, and P. Esquinazi, *Phys. Rev. B* **81**, 214414 (2010).
4. J. M. D. Coey et al., Surface magnetism of strontium titanate *J. Phys.: Condens. Matter*, **28**, 485001 (2016).
5. M. Hepting et al., Three-dimensional collective charge excitations in electron-doped copper oxide superconductors, *Nature* **563**, 374–378 (2018).
6. N. P. Armitage, P. Fournier, and R. L. Greene, Progress and perspectives on electron-doped cuprates, *Rev. Mod. Phys.* **82**, 2421 (2010).